Journal of BIOPHOTONICS

2-photon excitation fluorescence microscopy enables deeper high-resolution imaging of voltage and Ca2+ in intact mice, rat, and rabbit hearts

Journal:	*Journal of Biophotonics*
Manuscript ID:	jbio.201300109.R2
Wiley - Manuscript type:	Full Article
Date Submitted by the Author:	n/a
Complete List of Authors:	Ghouri, Iffath; University of Glasgow, Institute of Cardiovascular and Medical Sciences Kelly, Allen; University of Glasgow, Institute of Cardiovascular and Medical Sciences Burton, Francis; University of Glasgow, Institute of Cardiovascular and Medical Sciences Smith, Godfrey; University of Glasgow, Institute of Cardiovascular and Medical Sciences Kemi, Ole; University of Glasgow, Institute of Cardiovascular and Medical Sciences
Keywords:	Action Potential, Calcium, Deep Imaging, Myocardium, Two-Photon

2-photon excitation fluorescence microscopy enables deeper high-resolution imaging of voltage and Ca^{2+} in intact mice, rat, and rabbit hearts

Iffath A. Ghouri[1], Allen Kelly[1], Francis L. Burton[1], Godfrey L. Smith[1], Ole Johan Kemi*[,1]

[1]Institute of Cardiovascular and Medical Sciences; College of Medical, Veterinary, and Life Sciences; University of Glasgow, Glasgow, G12 8QQ, UK

*Corresponding author: E-mail: ole.kemi@glasgow.ac.uk, Phone: +44(0)1413305962, Fax: +44(0)1413305481

Short title: Ghouri et al.: Cardiac Live 2-Photon Microscopy

Keywords: action potential; calcium; deep imaging; myocardium; two-photon.

ABSTRACT

We describe a novel two-photon (2P) laser scanning microscopy (2PLSM) protocol that provides ratiometric transmural measurements of membrane voltage (V_m) via Di-4-ANEPPS in intact mouse, rat and rabbit hearts with subcellular resolution. The same cells were then imaged with Fura-2/AM for intracellular Ca^{2+} recordings. Action potentials (APs) were accurately characterized by 2PLSM vs microelectrodes, albeit fast events (<1ms) were sub-optimally acquired by 2PLSM due to limited sampling frequencies (2.6kHz). The slower Ca^{2+} transient (CaT) time course (>1ms) could be accurately described by 2PLSM. In conclusion, V_m- and Ca^{2+}-sensitive dyes can be 2P excited within the cardiac muscle wall to provide AP and Ca^{2+} signals to ~400µm.

Abstract Figure: 2P-excited images of Di-4-ANEPPS- and Fura-2/AM-loaded myocardium including the resultant AP and CaT extracted from the presented protocols.

1. Introduction

The cardiac action potential (AP) initiates myocardial contraction by activating an inward Ca^{2+} flux through the plasma membrane L-type Ca^{2+} channel. This Ca^{2+} influx stimulates ryanodine receptor-2-mediated Ca^{2+} release from the sarcoplasmic reticulum, which subsequently triggers sarcomere shortening and cardiac contraction. This excitation-contraction coupling process regulates the heartbeat on a beat-to-beat basis including variations in force generation and frequency and, if abnormalities occur, may also cause electric, systolic, and diastolic dysfunctions [1]. Transmural heterogeneities of the AP and intracellular Ca^{2+} handling have been investigated by computer simulations [2,3], deductions from transmural expression differences of associated proteins [4] and experimental observations by microelectrode or epifluorescence techniques [5-7]. However, the physiologic role of transmural heterogeneity remains incompletely understood. This is at least partly due to poor spatial resolution of the available optical fluorescence or electrical mapping techniques. In addition, tissue damage and loss of function may occur if studying biopsies or wedge preparations or if dissociating cardiomyocytes for isolated, single cell studies. Nonetheless, these studies have suggested that transmural heterogeneity generates a uniform workload across the ventricular wall during systole as well as diastole, but also that it may generate electrical disturbances and arrhythmias under pathologic conditions. Therefore, developing techniques that allow for measurements of APs and intracellular Ca^{2+} handling with high spatial and temporal resolution is important to understand characteristics of the cardiomyocyte under *in situ* physiologic conditions and to assess transmural differences of the intact heart. A combination of these measurements would also enable a better understanding of the relationship between voltage changes and Ca^{2+} fluxes.

Membrane voltage (V_m) and AP signals have traditionally been monitored using sharp microelectrodes. However, these measurements are limited to single, isolated cells, or to the epicardial surface of multicellular ventricular preparations. In contrast, V_m or intracellular Ca^{2+}-sensitive fluorescence dyes have enabled measurements of relative changes in whole hearts or ventricular preparations with widefield optical mapping or single-photon (1P) confocal laser scanning microscopy techniques [5,8,9], but these techniques are unable to discern the origin of the signal in the Z-axis as fluorescence is captured from a volume of hundreds of µm in depth (widefield mapping) or have been confined to a 30-50µm sample range along the Z-axis due to poor excitation and emission penetration (confocal) [10-11]. Thus, measurements of (sub)cellular events or transmural heterogeneities in whole-heart preparations have not been feasible.

The development of near infra-red 2-photon (2P) laser scanning microscopy (2PLSM) has enabled measurements from multi-cellular preparations with high penetration power (500-1,000µm), because of less light scattering compared to 1P wavelengths. Also, unlike 1P excitation confocal microscopy, 2P excitation requires the simultaneous absorption of 2 photons of longer wavelength (lower energy) light in order to excite a fluorophore. As the probability of absorption is proportional to the square of the instantaneous light intensity, lasers that generate ultra-short but intense pulses are used to provide a photon flux that confines excitation to an ellipsoidal volume around the focal point of the objective, whereas out-of-focus excitation and fluorescence emission is not generated [10]. As such, laser power may be increased as focal depth is increased in order to maintain signal, as out-of-focus signal does not interfere [10,11]. Thus, deep imaging of multi-cellular preparations with high spatial resolution optical sectioning including along the Z-axis is achieved without the need for a

detector pinhole (which is required in 1P excitation confocal microscopy to eliminate out-of-focus fluorescence emission), which further increases the fluorescence collection efficiency [11,12]. This, coupled with the availability of voltage- and Ca^{2+}-sensitive dyes that fluoresce after 2P excitation [13,14] allowed us to develop protocols for high-resolution deep imaging of AP and intracellular Ca^{2+} characteristics of *in situ* cardiomyocytes in intact, perfused whole hearts. These dyes include the aminonaphthylethenylpyridinium (ANEP) dyes, which bind to the plasma membrane of cells and undergo an emission spectral shift upon V_m changes [15], and Ca^{2+}-sensitive Fura dyes, which change excitation spectral properties relative to intracellular Ca^{2+}[16].

Here, we report novel protocols for high-fidelity 2PLSM measurements with high spatiotemporal resolution of cellular AP and intracellular Ca^{2+} handling characteristics of intact cardiomyocytes from defined regions of electrically stimulated and perfused left ventricle (LV) walls of whole hearts from mice, rats, and rabbits. These studies allow us to ascertain physiologic parameters from specific regions of interest within the myocardium, including transmural heterogeneities.

2. Experimental methods

For further details, see Supporting information online.

All procedures were approved by the Institutional Ethics Review Board and carried out in accordance with the *UK Animals (Scientific Procedures) Act 1986*. All chemicals were purchased from Sigma Aldrich, St. Louis, MO unless otherwise stated, whereas fluorescent dyes were purchased from Biotium, Hayward, CA or Molecular Probes, Life Technologies, Carlsbad, CA.

2.1 Spectral characterization of voltage- and Ca^{2+}-sensitive fluorescent dyes

Initial spectral characteristics of several voltage- (RH-237 and Di-4-ANEPPS) and Ca^{2+}-sensitive (Fluo-3, Calcium Green, Oregon Green, Rhod-2, and Fura-2) fluorescent dyes were obtained after 1P excitation spectrophotometry (LS55, Perkin Elmer, Shelton, CO) and 2P excitation by a Zeiss LSM 510 NLO upright microscope equipped with a 40x/0.8NA objective (Carl Zeiss, Jena, Germany), and a Ti:Sapphire 690-1040nm tunable laser (Chameleon, Coherent, Santa Clara, CA). Emission characteristics including spectral shifts of RH-237 and Di-4-ANEPPS during depolarization were also recorded in cardiomyocytes before and after depolarization with high extracellular K^+, by 488nm excitation with an Argon laser on an inverted confocal microscope (Zeiss LSM510 META, Carl Zeiss, Jena, Germany) equipped with a 40x/1.2NA objective, whereas emission was detected across the full emission spectrum by a 32 photomultiplier tube (PMT)-channel META detector; each channel covering a 10.7nm bandwidth. These experiments indicated that Di-4-ANEPPS for V_m and Fura-2 for intracellular Ca^{2+} presented with sufficiently distinct 2P spectral characteristics to provide distinct voltage and Ca^{2+} signals without crosstalk between the dyes; in line with previous experiments in our laboratory [13,14] and elsewhere [17,18], and were therefore used in the subsequent experiments.

2.2 AP recordings in isolated rabbit cardiomyocytes

To further investigate the response characteristics of Di-4-ANEPPS to changes in V_m, we clamped isolated single cardiomyocytes (see Supporting information online for cardiomyocyte isolation protocol) loaded with Di-4-ANEPPS (10µmol/L) using patch pipette microelectrodes pulled (Flaming/Brown P-97 Micropipette Puller, Sutter Instruments, Novato, CA) from borosilicate glass capillaries (Clark Electromedical, Oxford, UK) and filled with appropriate internal solutions. Initially, repeated voltage-clamp protocols were run, during which voltage was held at -80mV, stepped to -125mV, ramped over 1s to +85mV, and stepped back to -80mV (AxoClamp 2B Amplifier, Axon Instruments, Foster City, CA). Simultaneously, cells were 1P confocally excited with a 488nm Argon laser (Radiance 2000, BioRad, Hercules, CA) mounted to an inverted microscope (Nikon Eclipse, Nikon, Tokyo, Japan) equipped with a 60x/1.2NA objective, whereas fluorescence emission was captured in 510-560 and 610-650nm bandwidths, with the 2 output signals ratioed as they occur at either side of the emission peak (see below for explanation). Next, Di-4-ANEPPS-loaded cardiomyocytes were current-clamped and APs were elicited by 1nA, 5ms square pulses at 1Hz; APs were measured by microelectrodes and by epifluorescence (Optoscan, Cairn Research, Faversham, UK) recordings with excitation and emission wavelengths and light paths as described above (these experiments were performed by epifluorescence rather than confocal laser scanning measurements

to increase scan speed). These experiments were also repeated in the absence of Di-4-ANEPPS, and in the absence and presence of motion uncouplers 2,3-butanedione monoxime (BDM; 10mmol/L) and blebbistatin (10µmol/L; Enzo Life Sciences, Exeter, UK); no systematic effects were observed (data not shown). Isolated cardiomyocyte experiments were conducted by 1P excitation, as initial experiments indicated that 2P excitation quickly (~3s) killed dissociated cells or rendered cells dysfunctional, even at the lowest possible 2P laser power outputs (see example trace in Supporting figure 1). However, as indicated in Supporting figure 2A(i) and Figure 1, fluorescence emission does not differ between 1P and 2P excitation modes.

2.3 Microelectrode measurements of voltage in whole hearts

Membrane AP recordings from the epicardial surface of Langendorff-perfused rabbit, rat and mouse hearts (see Supporting information online for whole-heart preparation protocol) were obtained by positioning sharp microelectrodes onto the LV surface. Microelectrodes were pulled from borosilicate glass capillary pipettes with an internal diameter of 0.69mm as described above and filled with 1mol/L KCl (resistance ~40MΩ). Measurements were made using an Axoclamp 2B Amplifier and digitally recorded at a sampling frequency of 28kHz.

2.4 2P excitation measurements of voltage in whole hearts

Di-4-ANEPPS was prepared to a stock concentration of 2mmol/L in dimethyl sulfoxide (DMSO) and slowly perfused as a bolus (rabbit 100µL, rat 50µL, mouse 25µL) into the heart. Measurements were made using a 40x/0.8NA water-dipping objective on an upright Zeiss LSM 510 NLO microscope equipped with a Ti:Sapphire tunable laser (Figure 1A(i)). Di-4-ANEPPS was 2P excited at 920nm; emitted fluorescence was directed through a shortpass 685nm primary dichroic mirror and emission light split with a 580nm secondary dichroic mirror into wavelength bandwidths of 510-560nm (PMT1) and 590-685nm (PMT2), enabling a ratio of PMT1/PMT2 to be taken. For measurements of AP characteristics, high speed short line scans were performed to ensure maximum temporal resolution. Scan time was 0.382ms (~2.6kHz sampling frequency). For sequential voltage and Ca^{2+} measurements, high temporal resolution was not essential, so longer line scans (1.93ms, ~0.52kHz sampling frequency) were performed to maximize fluorescence signal and minimize fluorescence bleaching. Measurements of voltage were taken from 100µm below the LV epicardial surface and repeated at increasing depths through the myocardium at 100µm steps, down to ~500µm below the tissue surface.

2.5 2P excitation measurements of Ca^{2+} in whole hearts

Tyrode's solution for these experiments was supplemented with 1mmol/L probenecid to block anion transporters that excrete Fura-2, thus improving dye retention [19]. Fura-2/AM was prepared as a 1mmol/L stock in DMSO-pluronic acid F-127 (25% w/v). Boluses of dye (rabbit 250µL, rat 50µL, mouse 25µL) were injected into a bubble trap in the perfusion line to allow dilution of the dye and slow loading into the heart. Additional boluses of dye were injected if required due to low or time-

dependent loss of fluorescence signal. Fura-2/AM was 2P excited at 760nm (excited Fura-2 responsive to changes in Ca^{2+} concentration ([Ca^{2+}])) and 700nm (excited Fura-2 unresponsive to [Ca^{2+}]) to enable ratiometric processing of the fluorescence signal. Fluorescence emission was directed through a shortpass 685nm dichroic mirror and collected at 480-520nm (descanned detectors) or 505-545nm (non-descanned detectors) bandwidths. Ca^{2+} measurements through depth were made as described above, either immediately preceding or following voltage measurements (on the same line) in order to obtain sequential voltage and Ca^{2+} recordings.

2.6 Data analysis and statistics

AP recordings from 2P excitation and microelectrode measurements and intracellular Ca^{2+} transients (CaT) from 2P excitation were averaged and characterized in terms of 10-90% upstroke rise time (TRise) and duration of the AP from 50% activation to 90% repolarization (APD_{90}) or duration of the CaT from 50% activation to 90% decay (CaT_{90}). Images were processed using ImageJ. All data are expressed as mean±standard error of mean (SEM). Statistical analysis of the data was performed using paired student's t-test; a P-value of <0.05 was considered statistically significant.

3. Results and discussion

3.1 Spectral characterization of voltage-sensitive dye

Initial spectrophotometry of Di-4-ANEPPS confirmed that the dye primarily binds to the plasma membrane including transverse tubules of cardiomyocytes (Figure 1A(ii) and Supporting figure 2C(i)). Furthermore, power-corrected 2P excitation fingerprinting yielded peak emission after 920nm excitation (Figure 1A(ii) Insert); this coincided with the emission produced by the "doubled" 1P (1Px2) excitation spectrum (Supporting figure S2A(i)). The fluorescence emission spectrum was wide (500-700nm), but with a peak at ~580nm (Figure 1B(i) Insert), in line with that of the 1P excitation. Upon depolarization with extracellular KCl, a voltage-sensitive leftward spectral shift was observed, by which emission at shorter wavelength than the emission peak increased by 6-7%, whereas the emission at longer wavelengths than the peak decreased by ~2% (Figure 1B(i)). This allowed us to ratiometrically measure V_m, by collecting fluorescence emission in bands left (PMT1: 510-560nm; green band in Figure 1B(i)) and right (PMT2: 590-685nm; red band in Figure 1B(i)) of the emission peak. Figure 1B(ii) shows the individual emission bands imaged from an electrically twitch-stimulated rat heart (longitudinal line scan of a cardiomyocyte from the perfused whole-heart preparation, see arrow indicating line scan in Figure 1A(ii)). However, individual signals are prone to bleaching and motion artifacts, which are effectively abolished after ratiometric processing (PMT1/PMT2; see black trace in Figure 1B(ii)). These protocols were developed and validated in rabbit, rat, and mouse perfused whole-heart preparations (Figure 2), and used in the subsequent experiments.

Figure 1: A(i) Imaging setup of horizontal Langendorff perfused heart. **A(ii)** Example of a fluorescence image taken from a Di-4-ANEPPS-loaded rat myocardium at ~50µm depth; white arrow indicates approximate line scan location. Inset: 2P excitation fingerprinting for Di-4-ANEPPS revealed a peak excitation wavelength at 920nm. **B(i)** The emission spectrum of Di-4-ANEPPS was measured (inset). The spectral shift following depolarization of the cell membrane was characterized by taking a ratio of the fluorescence emission in the resting state with the emission following depolarization with high K^+. The wavebands at which light was collected by the two PMTs are shaded in green and red; the 580nm dichroic mirror used to split emission light is shown by the dashed line. **B(ii)** Averaged fluorescence measurements following a twitch-stimulus shows the opposite effects on fluorescence emission collected at PMT 1 (510-560nm, green trace) and PMT 2 (590-685nm, red trace). When ratioed (PMT 1/PMT 2), movement artifacts are cancelled out (black trace).

3.2 Comparison of 2P excitation and microelectrode AP and voltage recordings

We compared the performance of 2PLSM for recording APs with that of microelectrodes. Thus, perfused and paced hearts in which contraction was inhibited by blebbistatin and BDM to reduce motion artifacts were simultaneously loaded with Di-4-ANEPPS and impaled with sharp microelectrodes; both floating (also in the absence of contractile inhibitors) and fixed microelectrode configurations were used, with no differences occurring. Example traces of overlaid optical and microelectrode APs are presented in Figure 2A. Rabbit APD_{90}s were 133.4±7.1ms and

134.4±4.7ms after capture by 2PLSM and microelectrodes, whereas rat APD_{90}s were 51.6±6.8ms and 49.7±6.0ms and mouse APD_{90}s were 55.3±7.2ms and 50.7±4.1ms, respectively. Thus, these recordings indicated that APD_{90} was not different between 2PLSM and microelectrode recordings in any of the species, and also that the rabbit cardiac APD_{90} is longer compared to the rat and mouse cardiac APD_{90}, which are not different from one another (Figure 2C(i)). The species difference is explained by the lack of a plateau (phase 2) of the rodent AP and has been previously reported [1].

We also characterized and compared the ability to record AP upstrokes (phase 0) by 2PLSM versus microelectrodes (example traces in Figure 2B). TRise (10-90% of the upstroke) was not different between 2PLSM and microelectrode capture in rabbit hearts (2PLSM 2.88±0.30ms vs microelectrode 2.54±0.24ms). However, in rat and mouse hearts, TRise values obtained from microelectrode measurements were faster than those obtained by 2PLSM (0.50±0.05ms vs 0.92±0.13ms in rat; $p<0.05$ and 0.65±0.06ms vs 1.18±0.23ms in mouse; $p=0.065$, respectively; Figure 2C(ii)). It is possible the faster TRise values obtained by microelectrodes vs 2PLSM in rodents, in which the AP upstroke is a sub-ms event, is explained by the comparatively faster sampling frequency of 28kHz vs that of 2PLSM (2.6kHz). Thus, we sub-sampled AP data recorded by microelectrodes from 28kHz to 2.8kHz to match 2P sampling frequencies. This reduced the difference in TRise values (sub-sampled microelectrode recordings: rat 0.70±0.02ms and mouse 0.78±0.03ms) and eliminated any significant differences from 2PLSM recordings ($p>0.05$; Figure 2C(ii)).

We investigated the response characteristics of Di-4-ANEPPS to changes in V_m, by voltage-clamping isolated rabbit Di-4-ANEPPS-loaded cardiomyocytes with patch micropipettes and thereafter ramping voltage from -125mV to +85mV over 1s, including initial and subsequent stepping from and to -80mV. Cells were 1P confocally excited at 488nm throughout and fluorescence emission was ratiometrically captured in 510-560nm and 610-650nm bandwidths. 1P excitation was used as 2P excitation quickly induces irreversible damage to single isolated cells (Supporting figure 1) and as 1P and 2P fluorescence emissions do not differ (Figure 1 and Supporting figure 2A(i)). As seen in Supporting Figure 3A, ratiometric fluorescence emission closely followed changes in V_m. Next, APs were elicited in current-clamped and Di-4-ANEPPS-loaded cardiomyocytes, with APs measured by microelectrodes and by epifluorescence at high temporal resolution. These experiments showed that elicited APs were faithfully captured by ratiometric Di-4-ANEPPS fluorescence recordings with high spatiotemporal resolution (Supporting figure 3B(i)), including during the upstroke and the initial charging phase (Supporting figure 3B(ii)).

Figure 2: A Example single AP recordings made by microelectrode (dark trace) and 2P (light trace) methods from **(i)** rabbit, **(ii)** rat and **(iii)** mouse hearts. **B** Original (dark gray trace) and sub-sampled (mid-gray trace) microelectrode and 2P (light gray trace) AP upstroke recordings from the same **(i)** rabbit, **(ii)** rat and **(iii)** mouse hearts. **C(i)** APD_{90} and **C(ii)** TRise values obtained by microelectrode and 2P methods were compared, including TRise from sub-sampled microelectrode recordings. n=4 for rabbit and mouse, n=3 for rat. *$p<0.05$.

3.3 Spectral characterization and application of Ca^{2+}-sensitive dyes

Initial spectral characterization of Ca^{2+}-sensitive dyes (data not shown) confirmed that Fura-2 was both excitable with 2PLSM and presented with emission spectra discernible from Di-4-ANEPPS, such that intracellular Ca^{2+} and V_m could be measured without cross-contamination of voltage and Ca^{2+} signals. As the 1P Fura-2 excitation spectrum is in the ultraviolet range with an absorption shift caused by changes in free Ca^{2+} [16,20], we obtained 2P excitation spectra of Fura-2 at both high (60µmol/L) and low (>1nmol/L) free Ca^{2+}, and compared these to the doubled 1P spectra (1Px2). As seen in Supporting figure 2A(ii), the absorption shift produced by high Ca^{2+} also leads to a leftward shift in the 1Px2 spectra. On 2P excitation, a slightly red-shifted excitation spectrum appeared with a peak at 760nm at low Ca^{2+}. At high Ca^{2+}, only the right tail of a Ca^{2+}-sensitive spectrum could be obtained, with no peak discernible (Supporting figure 2A(ii)), indicating that the 2P excitation peak of Fura-2 in high Ca^{2+} occurs at <690nm. Since intracellular free Ca^{2+} occurs in the range 0.1-1µmol/L, we decided to further characterize the feasibility of Ca^{2+}-sensitive 2P excitation of Fura-2 at 760nm. This wavelength is compatible with sequential 2P imaging of V_m after simultaneous loading with Di-4-ANEPPS, of which excitation spectrum appears above and out with 760nm (Supporting figure 2B(i)), ensuring minimal cross-contamination. To confirm this, we loaded isolated cells with both Di-4-ANEPPS and Fura-2/AM before 2P excitation fingerprinting from 690nm to 1040nm (Supporting figure 2B(ii)). This demonstrated separate excitation peaks for Fura-2 and Di-4-ANEPPS, respectively; see the dashed vertical lines for 2P excitation wavelengths used for Fura-2 (black) and Di-4-ANEPPS (red). Supporting figure 2C shows a single isolated cardiomyocyte loaded with both Di-4-ANEPPS and Fura-2/AM after sequential excitation at 920nm (i) and 760nm (ii), indicating that fluorescence emission after 920nm excitation originates from the plasma membrane and transverse tubules, whereas fluorescence emission after 760nm excitation originates from the cytoplasm.

In order to also establish 2PLSM protocols for measuring intracellular Ca^{2+} in Fura-2/AM-loaded beating hearts, we measured fluorescence emission after 2P excitation at wavelengths 690-860nm in the perfused whole-heart preparation, while discriminating between diastolic and systolic signals as obtained during continuous electrical pacing-evoked trains of Ca^{2+}-transients. Figure 3A(i) shows the averaged fluorescence emission values during diastole (black) and systole (light gray) for this range of excitation wavelengths. A ratio of these fluorescence values was subsequently taken ($F_{systole}/F_{diastole}$; gray) in order to indicate the excitation wavelength that produced the greatest relative change in fluorescence emission in response to changes in intracellular [Ca^{2+}]. This occurred at the excitation wavelength 760nm. Thus, at 760nm 2P excitation, Fura-2/AM fluorescence emission decreases when intracellular Ca^{2+} increases (Figure 3A(ii)). This is in line with the response pattern to 1P excitation at 380nm (to the right of the isosbestic point), which is normally ratioed with emission after 340nm excitation (to the left of the isosbestic point) [13,14,16]. A corresponding 2P excitation (1Px2) for 340nm; i.e. to the left of the isosbestic point, could not be performed due to 2P laser tuning limitations, but 2P excitation at 700nm was found to produce virtually no difference between systolic and diastolic fluorescence (Figure 3A(ii)). This suggests that 700nm is at or very close to the isosbestic point for Fura-2-free Ca^{2+} interaction during 2P excitation, in agreement with previous work [21]. As such, sequential imaging with excitation wavelengths 700nm (Ca^{2+}-insensitive) and 760nm (Ca^{2+}-sensitive) allows for ratiometric 2P measurements of intracellular Ca^{2+} in whole-hearts. Figure 3A(ii) shows the captured intracellular CaT in a twitch-stimulated and perfused Fura-2/AM-loaded rat heart. Similar fluorescence characteristics were observed after 2P excitation at 700nm and 760nm wavelengths in mouse and rabbit hearts (Supporting figure 4),

enabling ratiometric Ca^{2+} measurements to be made in all species tested. However, it should be pointed out that ratiometric processing of the fluorescence signals obtained from 760nm and 700nm excitations does not achieve the same ability to resolve motion artifacts as for AP and V_m recordings, as the ratioed Fura-2 (Ca^{2+}) signals stem from different excitation periods.

CaT characteristics were quantified with respect to duration and rise time of the upstroke. The CaT time from activation to 90% decay (CaT_{90}) differed between species; from a CaT_{90} of 235±15ms in rabbit to 97±3ms in mouse hearts (Figure 3B(i)); however, different pacing cycle lengths were used between the species, as indicated by the dashed lines, whereas the 10-90% time to peak did not differ (6-8ms; Figure 3B(ii)).

Figure 3: A(i) Mean diastolic (black trace) and systolic (red trace) fluorescence emission at 2P excitation wavelengths 690-860nm in twitch-stimulated Fura-2/AM-loaded rat hearts (emission collected at 480-520nm). Mean systolic/diastolic fluorescence ratio (dotted gray trace) identified the excitation wavelength (760nm) producing the greatest %-change in fluorescence levels in response to changes in [Ca^{2+}]. **(ii)** Fluorescence emission during a single twitch-stimulation at 2P excitation 760nm (black trace) and 700nm (light gray trace; with virtually no difference between systolic and diastolic fluorescence levels). Ratiometric measurements of intracellular CaTs could therefore be taken using these two excitation wavelengths (700nm/760nm; gray trace). **B(i)** Mean CaT_{90} for rabbit, rat and mouse. The dashed lines above the columns represent the pacing cycle lengths for each species. **(ii)** Mean CaT TRise for rabbit, rat and mouse. n=3 for each species.

3.4 Sequential AP and Ca^{2+} recordings by 2PLSM

After establishing spectrally distinct protocols for 2PLSM measurements of V_m (Di-4-ANEPPS) and intracellular Ca^{2+} (Fura-2/AM) in perfused and twitch-stimulated whole-heart preparations, we next loaded the hearts with both fluorescent indicators Di-4-ANEPPS and Fura-2/AM simultaneously. Due to different excitation wavelengths, truly simultaneous 2P excitation was not feasible, but sequential excitation was, with change-over time in the order of seconds, as dictated by the tuning of the 2P Ti:Sapphire laser. Thus, we 2P excited the rat heart first at 920nm (Di-4-ANEPPS; Figure 4A(i)), secondly at 760nm, and thirdly at 700nm (Fura-2/AM; Figure 4A(ii)), with emission filters as described above to set up recordings for both dyes. V_m- and intracellular Ca^{2+}-sensitive signals were then line scan recorded using the same line longitudinal to the cardiomyocyte bundle direction (white arrow in Figures 4A(i) and (ii)). These recordings yielded optical APs and CaTs (Figure 4A(iii)) with similar shape and signal-to-noise ratio (SNR) characteristics as in the recordings with only one fluorescent dye present. This was also achieved for mouse (Figure 4B) and rabbit (Figure 4C) hearts. Thus, sequential recordings of V_m and intracellular Ca^{2+} were achieved with no apparent cross-contamination, deterioration, or loss of signal quality. However, inhibiting myocardial contraction remains important to avoid shifting of the area being recorded.

Figure 4A also indicates that in the whole-heart preparation, Di-4-ANEPPS loaded primarily to the plasma membrane and transverse tubules and that Fura-2/AM loaded homogeneously to the

intracellular space of cardiomyocytes, in line with enzymatically isolated cardiomyocytes (Supporting figure 2C).

Figure 4: A Example images showing sequential 2P excitation of **(i)** Di-4-ANEPPS (920nm) and **(ii)** Fura-2/AM (760nm) in a rat heart preparation. White arrows indicate the line scan direction parallel to fiber orientation. **(iii)** Sequential Di-4-ANEPPS V_m (black trace) and Fura-2/AM intracellular CaT (red trace) line scan recordings from the same preparation. Intracellular Ca^{2+} measurement were also made in Langendorff perfused **(B)** mouse and **(C)** rabbit hearts. **(i)** Fura-2 measurements exciting at 760nm (black trace) and 700nm (gray trace) enabled ratiometric processing of the emitted fluorescence (F_{700}/F_{760}); **ii)**. Sequential recordings of Di-4-ANEPPS for V_m (black trace) and Fura-2/AM for CaT (gray trace) from mouse and rabbit hearts **(iii)**.

SNR as well as signal accuracy during fast events may vary with different line scan speeds. We investigated this by 2P imaging APs and intracellular CaTs using both fast (0.382ms scan time/line) and slow (1.93ms scan time/line) line scan sampling frequencies. For AP measurements, the slower line scan speed improved the SNR and did not affect APD_{90}, but did not capture data sufficiently fast to accurately record the fast AP upstroke (Supporting figure 4A). SNR for CaT measurements was also improved by a slow line scan speed, but without affecting the capture of either CaT_{90} or TRise of the CaT (Supporting figure 4B). This is likely explained by the slower upstroke characteristics of the CaT vs the AP [1]. Thus, 2PLSM provides a sensitive measurement of physiologic events in the ms range, but the scan rate may be insufficient for accurately resolving fast events in the sub-ms range. Here, this affected the ability to resolve AP upstrokes in rodents; a <1ms event, as indicated by the microelectrode measurements and as previously reported [20]. Thus, the temporal resolution of the current 2PLSM protocols is not comparable to sampling rates offered by e.g. microelectrode set-ups (10-fold faster). Reducing the sampling area by shortening the line scan may mitigate this, since it is not caused by dye response rates.

3.5 Transmural AP and Ca^{2+} recordings by 2PLSM

In order to characterize APs and intracellular CaTs transmurally from the surface to the deep myocardium, we line scan imaged in 100µm steps along the Z-axis. This consistently allowed for recordings down to ~500µm depths, with discernible APs (Figure 5A(i) and 5B(i)) and CaTs (Figure 5A(ii) and 5B(ii)). This is ~10-fold deeper than achieved by confocal 1P imaging [9]. However, deep imaging was associated with a gradual loss of signal and a concomitant reduction in SNR from both fluorescent indicators (Figure 5C; from ~4-7 at 100µm depth to 1-1.5 at 500µm depth). Nonetheless, despite reduced signal intensity and quality, the AP and CaT characteristics remained virtually unchanged through the transmural myocardium (Figure 5), as also indicated by previous efforts [18]. As such, information about structure could not be obtained from deep layers, whereas V_m- and intracellular Ca^{2+}-sensitive signals were still obtained. It is possible tissues with less light scattering, more powerful or longer wavelength lasers, more efficient light transmission by improved optics including lens selection, or more sensitive light capture may allow imaging at deeper layers [10,22].

Nonetheless, the current protocols enable live imaging of defined subcellular areas across the transmural myocardium of the intact, perfused, and paced heart of several species with high spatiotemporal resolution. This allows for detailed and mechanistic studies of phenomena that are not resolved by measurements based on microelectrode, 1P confocal, or surface mapping of epifluorescence, or by isolated single cell studies. This includes studies of transmural heterogeneities present in the mammalian heart [2-7] and other spatially distinct events.

Figure 5: (i) Di-4-ANEPPS and **(ii)** Fura-2/AM recordings from **(A)** 100µm and **(B)** 400µm depths of the rat myocardium. **C** The average SNR decreased with depth for both Di-4-ANEPPS (dark trace) and Fura-2/AM (light trace).

3.6 2P recordings from non-myocardial tissue

Finally, we investigated in more detail the characteristics of fluorescence emission from incremental depths including its propagation across non-myocardial structures. For this, Z-stacks of XY-images were taken with incremental 1µm steps between images from Di-4-ANEPPS-loaded myocardial tissue of a heart preparation (Figure 6(i)). The composite XZ-image indicates the presence of a circular blood vessel embedded in the myocardium that is void of di-4-ANEPPS fluorescence. This is indicated in more detail in Supporting figure 5A, showing a loss of signal corresponding to the lumen of the blood vessel. First, we line scan imaged across the blood vessel including the adjacent myocardium (along the arrow in Supporting figure 5A(i)) in order to record APs. APs were obtained by 2PLSM as described above; Supporting figure 5B(i) shows the ratio signal, in which optical APs can be clearly observed from the myocardial tissue (Supporting figure 5B(ii) and Supporting figure 5B(iv)), whereas the ratio signal from the blood vessel lumen also indicates presence of faint optical APs (Supporting figure 5B(i); signal between the dotted vertical lines) and Supporting figure 5B(iii). However, since the signal intensity from the blood vessel is equally compromised in both PMT channels (Supporting figure 5A(ii), the ratio signal appears to have an AP signal of approximately normal amplitude, but with a dramatic increase in noise (Supporting figure 5B(iii)), compared to the myocardium (Supporting figure 5C). This is consistent with lack of a membrane to which Di-4-ANEPPS may bind as well as the loss of electrical activity in the blood vessel. A closer inspection also indicates that any residual AP-like signal in the blood vessel lies closer to the vessel wall rather than the mid-lumen (Supporting figure 5B(i)), indicating the origin of the signal is not the lumen itself, but rather caused by scattering and/or dispersion of the fluorescence emitting from adjacent myocardium, which may be especially pronounced along the Z-axis [23].

This was investigated in more detail by tracking the AP wave front through the myocardium including through a blood vessel during an endocardial-to-epicardial activation cycle (Figure 6); achieved by right atrial pacing, from which ventricular transmural activation propagates through the myocardium with a direction from the endocardium to the epicardium [24]. This activation direction was confirmed by the recorded activation times through the 150µm Z-stack of XY-images that was obtained from an area of the Di-4-ANEPPS-loaded heart with a blood vessel present in the myocardium (Figure 6(i); see confirmation in XY-planes above (Figure 6(ii), at level (Figure 6(iii), and below (Figure 6(iv) the blood vessel). The right atrial paced endocardial-to-epicardial AP conduction direction enabled the likely origin of the V_m signal obtained from the blood vessel to be determined from the activation times. The activation delay increased from the deepest section toward the

epicardial surface (Figure 6(i)). It is noteworthy that the apparent signal from the blood vessel lumen had an activation time faster than adjacent myocardial tissue on the same plane, and considerably faster activation time than the overlying epicardial myocardium. This suggests the signals in the blood vessel are arising from deeper layers in the endocardial direction. Thus, activation wave front mapping confirmed that the signal obtained in the blood vessel lumen was arising from deeper, underlying layers of the myocardium. Thus, care should be taken when interpreting signals from the deep myocardium due to deterioration of axial resolution, especially as this may be non-uniform due to structural heterogeneity.

Figure 6: (i) A Z-stack (150 slices at 1µm intervals) was used to reconstruct an XZ-image of the Di-4-ANEPPS-loaded mouse epicardium/myocardium containing a blood vessel (epicardial surface at the top of the image). Average activation times (in ms) relative to the shortest activation time obtained from sections of the scan line above, through, and below the blood vessel after right atrial pacing with an endocardial-to-epicardial activation wave front direction (indicated by the black arrow). The locations from where the activation times were obtained are indicated by the solid and dashed lines. XY-images from the Z-stack of the different layers above **(ii)**, through **(iii)**, and below **(iv)** the blood vessel from where the line scans were taken are inserted.

4. Conclusions

Current methods for assessing electrical activity and Ca^{2+} cycling across the intact transmural myocardium suffer with respect to ascertaining the origin of the signal or with regard to resolving spatially accurate signals from depths below the surface of the preparation (see Introduction). These inadequacies may be overcome by 2PLSM. As such, a new line of studies has started to develop 2PLSM protocols to investigate electrical activity [25] or Ca^{2+} signaling [17,26,27] in intact heart preparations, but to our knowledge, our study is the first to measure V_m and intracellular Ca^{2+} in the same preparation by 2PLSM near-simultaneously. Thus, we describe novel protocols that enable ratiometric 2P measurements of cellular V_m and therefore electrical activation, as well as intracellular Ca^{2+} cycling after simultaneous loading of the respective fluorescent dyes Di-4-ANEPPS and Fura-2/AM. These protocols enable sequential recordings of APs and intracellular CaTs with subcellular resolution within distinct and defined deep layers of the intact, perfused whole-heart preparation. Previous [10,13,23] and current studies indicate a spatiotemporal resolution of ~0.5x0.5x2.5µm (XYZ) and ~1ms. For validation, we compared signals of fast events obtained by 2PLSM to those of 28kHz microelectrodes in both isolated cells and intact hearts, and we extended the protocols to a range of species commonly used in basic heart research.

Strengths: Since Di-4-ANEPPS and Fura-2/AM compartmentalize to different cellular areas [15,16,28], the simultaneous presence in the preparation does not noticeably affect the individual measurements compared to loading with one dye alone. Furthermore, because of the ratiometric nature of the imaging, effects of heterogenic dye loading and motion artifacts that may occur during excitation-contraction coupling may be minimized, and dye loading may be repeated during prolonged experiments. In fact, because of wash-out, photobleaching, and gradual internalization to the cell in the case of Di-4-ANEPPS [26], repeated dye loading may be necessary during prolonged experiments. However, both Di-4-ANEPPS and Fura-2 are resistant to photobleaching and present with an appropriate sensitivity to changes in V_m (Di-4-ANEPPS) and intracellular Ca^{2+} (Fura-2) [15,16]. A high sensitivity of Di-4-ANEPPS to changes in V_m was confirmed in the present study, whereas Fura-2 has a dissociation constant to free Ca^{2+} of 224nM in the presence of 1mM Mg^{2+} [16], which is close to diastolic intracellular [Ca^{2+}] in cardiomyocytes (150-300nM) [1]. This makes Di-4-ANEPPS and Fura-2/AM amenable to prolonged experiments in cardiac preparations, which coupled with the minimally invasive nature of 2P excitation [10-12] precedes other available techniques.

Limitations: Because 2P excitation is limited to one wavelength at any given time, the recordings of V_m (AP) and intracellular Ca^{2+} (CaT) may not be performed simultaneously, only sequentially, with a time of ~5s associated with tuning of the 2P excitation laser and accompanying filter set shifting. The use of two excitation wavelengths for Fura-2/AM-based Ca^{2+} measurements further compounds this. Also, uncoupling contraction from excitation and Ca^{2+} release is necessary for the current protocols; achieved by BDM and blebbistatin, but this may confound the morphology of APs and CaTs, especially in the whole-heart preparation [29], although minimal effects of BDM [30] and blebbistatin [31] have also been reported.

Acknowledgements

The authors would like to thank Aileen Rankin and Mike Dunne for expert technical assistance and Dr Niall MacQuaide and Dr Sarah Kettlewell for help with supporting figures.

This work was supported by a European Union Framework Programme 7 grant (HEALTH-F2-2009-241526) and a British Heart Foundation project grant.

References

[1] D.M. Bers. Nature **415**, 198-205 (2002).

[2] V.E. Bondarenko, and R R.L. Rasmusson. Am. J. Physiol. Heart Circ. Physiol. **299**, H454-H469 (2010).

[3] E. Hermeling, T.M. Verhagen, F.W. Prinzen, and N.H.L. Kuijpers. Comput. Cardiol. **36**, 397-400 (2009).

[4] K.R. Laurita, R. Katra, B. Wible, X. Wan, and M.H. Koo. Circ. Res. **92**, 668-675 (2003).

[5] B.R. Choi, and G. Salama. J. Physiol. **529**, 171-188 (2000).

[6] V.M. Figueredo, R. Brandes, M.W. Weiner, B.M. Massie, and S.A. Camacho. Circ. Res. **72**, 1082-1090 (1993).

[7] S.C. Verduyn, J.G.M. Jungschleger, M. Stengl, R.L.H.M.G. Spatjens, J.D.M. Beekman, and M.A. Vos. Pflugers. Arch. Eur. J. Physiol. **449**, 115-122 (2004).

[8] H. Nishizawa, T. Suzuki, T. Shioya, Y, Nakazato, H. Daida, and N. Kurebayashi. PLoS. One **4**, e7069 (2009).

[9] G.L. Aistrup, Y. Shiferaw, S. Kapur, A.H. Kadish, and J.A. Wasserstrom. Circ. Res. **104**, 639-649 (2009).

[10] F. Helmchen, and W. Denk. Nat. Methods **2**, 932-940 (2005).

[11] V.E. Centonze, and J.G. White. Biophys. J. **75**, 2015-2024 (1998).

[12] M. Rubart. Circ. Res. **95**, 1154-1166 (2004).

[13] G.L. Smith, M. Reynolds, F.L. Burton, and O.J. Kemi. Methods Cell. Biol. **99**, 225-261 (2010).

[14] D.L. Wokosin, C.M. Loughrey, and G.L. Smith. Biophys. J. **86**, 1726-1738 (2004).

[15] E. Fluhler, V.G. Burnham, and L.M. Loew. Biochemistry **24**, 5749-5755 (1985).

[16] G. Grynkiewicz, M. Poenie, and R.Y. Tsien. J. Biol. Chem. **260**, 3440-3450 (1985).

[17] J. Mutze, V. Iyer, J.J. Macklin, J. Colonell, B. Karsh, Z. Petrasek, P. Schwille, L.L. Looger, L.D. Lavis, and T.D. Harris. Biophys. J. **102**, 934-944 (2012).

[18] M. Rubart, E. Wang, K.W. Dunn, and L.J. Field. Am. J. Physiol. Cell. Physiol. **284**, C1654-C1668 (2003).

[19] F. Divirgilio, C. Fasolato, and T.H. Steinberg. Biochem. J. **256**, 959-963 (1988).

[20] H. Windisch, W. Muller, and H.A. Tritthart. Biophys. J. **48**, 877-884 (1985).

[21] 2P excitation spectra Fura-2: http://www.drbio.cornell.edu/cross_sections.html

[22] L. Sacconi, D.A. Dombeck, and W.W. Webb. Proc. Natl. Acad. Sci. USA. **103**, 3124-3129 (2006).

[23] W.R. Zipfel, R.M. Williams, and W.W. Webb. Nature Biotechnol. **21**, 1369-1377 (2003).

[24] P. Helm, M.F. Beg, M.I. Miller, and R.L. Winslow. Ann. N. Y. Acad. Sci. **1047**, 296-307 (2005).

[25 J. Dumas, and S. Kinisley. Ann. Biomed. Eng. **33**, 1802-1807 (2005).

[26] R.J. Hassink, K.B. Pasumarthi, H. Nakajima, M. Rubart, M.H. Soonpaa, A.B. de la Riviere, P.A. Doevendans, and L.J. Field. Cardiovasc. Res. **78**, 18-25 (2008).

[27] N. Smart, S. Bollini, K.N. Dube, J.M. Vieira, B. Zhou, S. Davidson, D. Yellon, J. Riegler, A.N. Price, M.F. Lythgoe, W.T. Pu, and P.R. Riley. Nature **474**, 640-644 (2011).

[28] A. Bullen, and P. Saggau. Biophys. J. **76**, 2272-2287 (1999).

[29] K.E. Brack, R. Narang, J. Winter, and G.A. Ng. Exp. Physiol. **98**, 1009-1027 (2013).

[30] S. Kettlewell, N.L. Walker, S.M. Cobbe, F.L. Burton, and G.L. Smith. Exp. Physiol. **89**, 163-172 (2004).

[31] V.V. Fedorov, I.T. Lozinsky, E.A. Sosunov, E.P. Anyukhovsky, M.R. Rosen, C.W. Balke, and I.R. Efimov. Heart Rhythm **4**, 619-626 (2007).

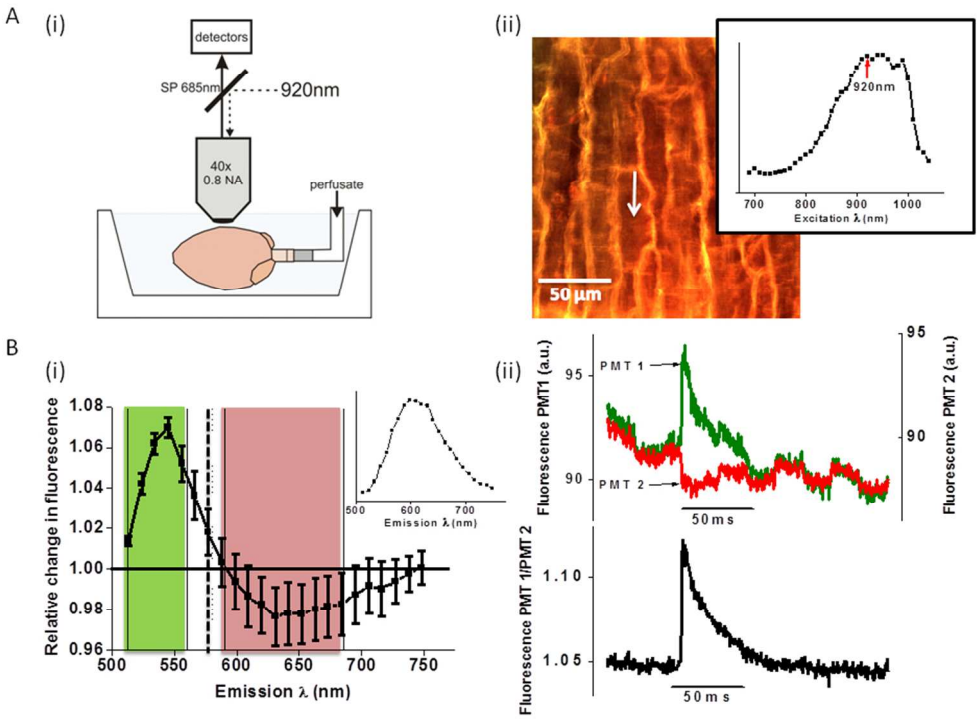

Figure 1: A(i) Imaging setup of horizontal Langendorff perfused heart. A(ii) Example of a fluorescence image taken from a Di-4-ANEPPS-loaded rat myocardium at ~50µm depth; white arrow indicates approximate line scan location. Inset: 2P excitation fingerprinting for Di-4-ANEPPS revealed a peak excitation wavelength at 920nm. B(i) The emission spectrum of Di-4-ANEPPS was measured (inset). The spectral shift following depolarization of the cell membrane was characterized by taking a ratio of the fluorescence emission in the resting state with the emission following depolarization with high K+. The wavebands at which light was collected by the two PMTs are shaded in green and red; the 580nm dichroic mirror used to split emission light is shown by the dashed line. B(ii) Averaged fluorescence measurements following a twitch-stimulus shows the opposite effects on fluorescence emission collected at PMT 1 (510-560nm, green trace) and PMT 2 (590-685nm, red trace). When ratioed (PMT 1/PMT 2), movement artifacts are cancelled out (black trace). 254x190mm (96 x 96 DPI)

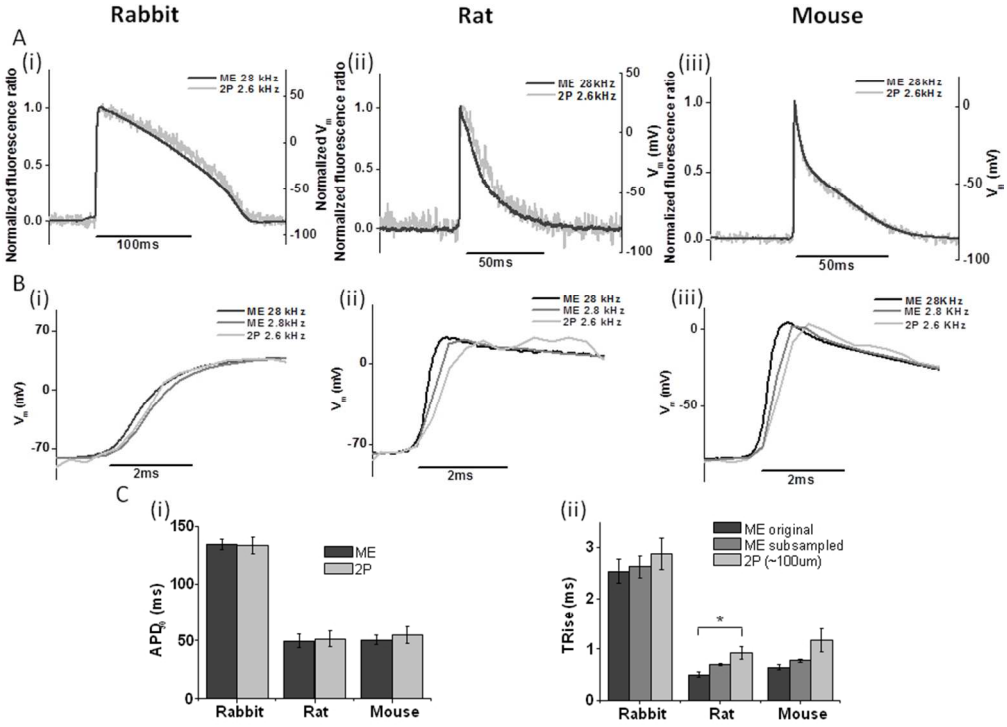

Figure 2: A Example single AP recordings made by microelectrode (dark trace) and 2P (light trace) methods from (i) rabbit, (ii) rat and (iii) mouse hearts. B Original (dark gray trace) and sub-sampled (mid-gray trace) microelectrode and 2P (light gray trace) AP upstroke recordings from the same (i) rabbit, (ii) rat and (iii) mouse hearts. C(i) APD90 and C(ii) TRise values obtained by microelectrode and 2P methods were compared, including TRise from sub-sampled microelectrode recordings. n=4 for rabbit and mouse, n=3 for rat. *p<0.05.
254x190mm (96 x 96 DPI)

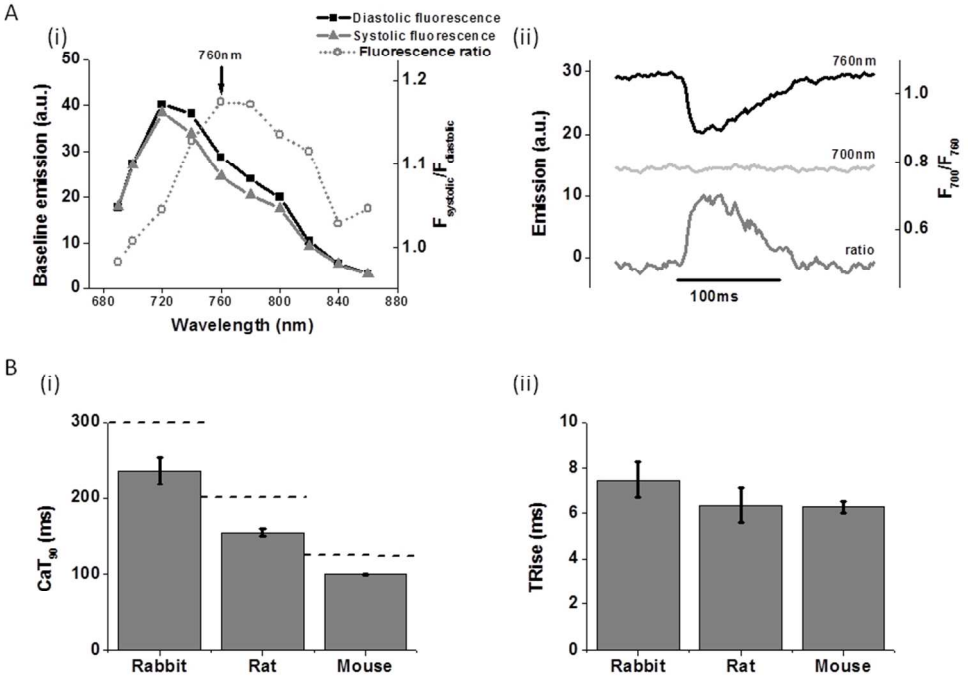

Figure 3: A(i) Mean diastolic (black trace) and systolic (red trace) fluorescence emission at 2P excitation wavelengths 690-860nm in twitch-stimulated Fura-2/AM-loaded rat hearts (emission collected at 480-520nm). Mean systolic/diastolic fluorescence ratio (dotted gray trace) identified the excitation wavelength (760nm) producing the greatest %-change in fluorescence levels in response to changes in [Ca2+]. (ii) Fluorescence emission during a single twitch-stimulation at 2P excitation 760nm (black trace) and 700nm (light gray trace; with virtually no difference between systolic and diastolic fluorescence levels). Ratiometric measurements of intracellular CaTs could therefore be taken using these two excitation wavelengths (700nm/760nm; gray trace). B(i) Mean CaT90 for rabbit, rat and mouse. The dashed lines above the columns represent the pacing cycle lengths for each species. (ii) Mean CaT TRise for rabbit, rat and mouse. n=3 for each species.
254x190mm (96 x 96 DPI)

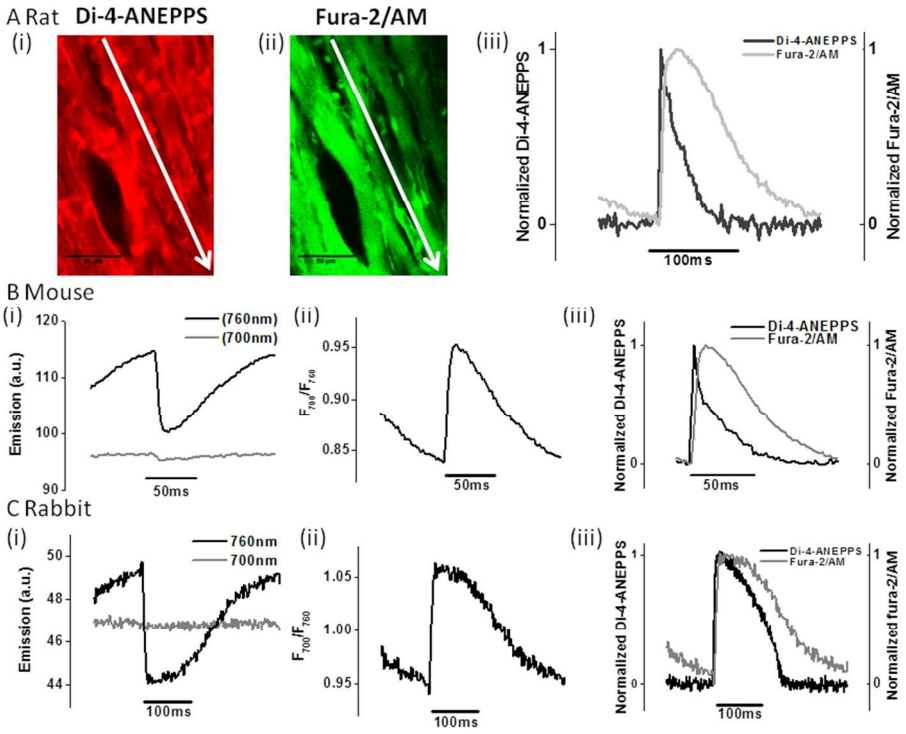

Figure 4: A Example images showing sequential 2P excitation of (i) Di-4-ANEPPS (920nm) and (ii) Fura-2/AM (760nm) in a rat heart preparation. White arrows indicate the line scan direction parallel to fiber orientation. (iii) Sequential Di-4-ANEPPS Vm (black trace) and Fura-2/AM intracellular CaT (red trace) line scan recordings from the same preparation. Intracellular Ca2+ measurement were also made in Langendorff perfused (B) mouse and (C) rabbit hearts. (i) Fura-2 measurements exciting at 760nm (black trace) and 700nm (gray trace) enabled ratiometric processing of the emitted fluorescence (F700/F760); ii). Sequential recordings of Di-4-ANEPPS for Vm (black trace) and Fura-2/AM for CaT (gray trace) from mouse and rabbit hearts (iii).
254x190mm (96 x 96 DPI)

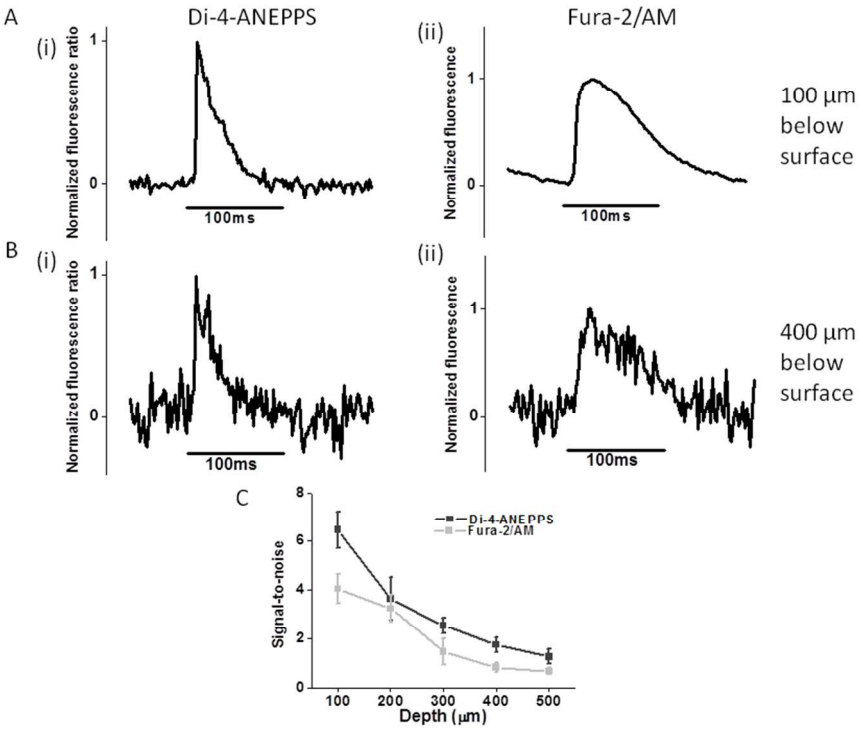

Figure 5: (i) Di-4-ANEPPS and (ii) Fura-2/AM recordings from (A) 100µm and (B) 400µm depths of the rat myocardium. C The average SNR decreased with depth for both Di-4-ANEPPS (dark trace) and Fura-2/AM (light trace).
254x190mm (96 x 96 DPI)

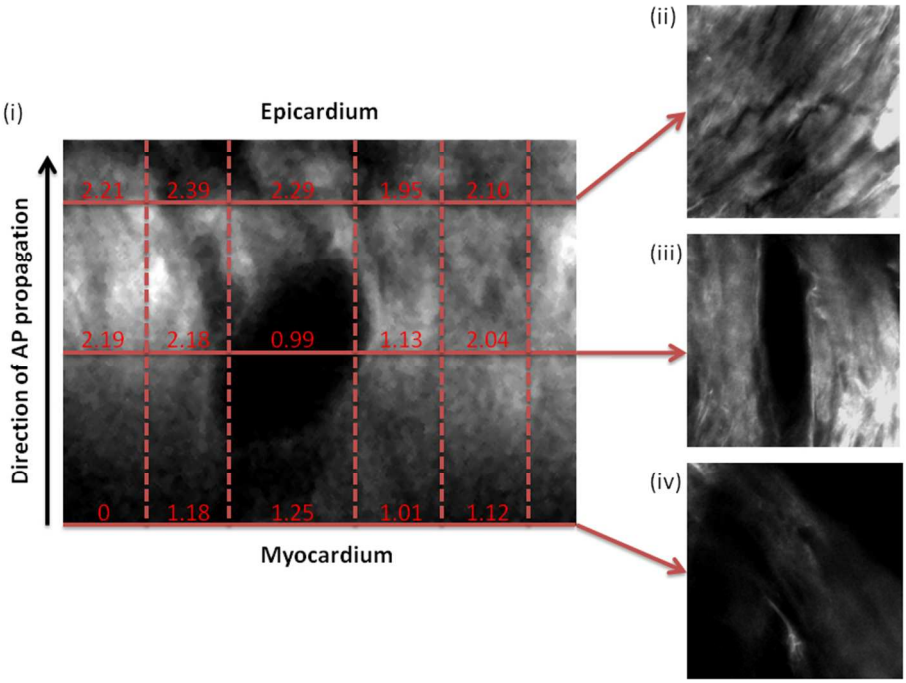

Figure 6: (i) A Z-stack (150 slices at 1µm intervals) was used to reconstruct an XZ-image of the Di-4-ANEPPS-loaded mouse epicardium/myocardium containing a blood vessel (epicardial surface at the top of the image). Average activation times (in ms) relative to the shortest activation time obtained from sections of the scan line above, through, and below the blood vessel after right atrial pacing with an endocardial-to-epicardial activation wave front direction (indicated by the black arrow). The locations from where the activation times were obtained are indicated by the solid and dashed lines. XY-images from the Z-stack of the different layers above (ii), through (iii), and below (iv) the blood vessel from where the line scans were taken are inserted.
254x190mm (96 x 96 DPI)

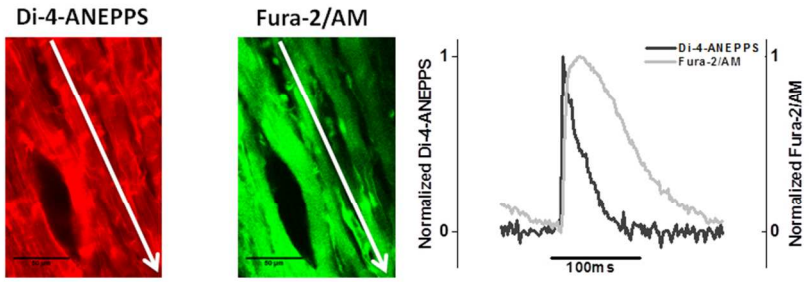

Abstract Figure: 2P-excited images of Di-4-ANEPPS- and Fura-2/AM-loaded myocardium including the resultant AP and CaT extracted from the presented protocols.
254x190mm (96 x 96 DPI)